Journal of Environmental Radioactivity 251–252 (2022) 106978

Contents lists available at ScienceDirect

Journal of Environmental Radioactivity

journal homepage: www.elsevier.com/locate/jenvrad

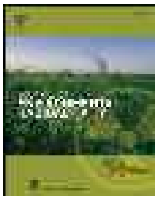

# Microscale spatial variability of Beryllium-7 at a reference site in southwest China

Zhonglin Shi [a,*], William H. Blake [b], Jin Guo [c], Yi Long [a], Anbang Wen [a]

[a] Institute of Mountain Hazards and Environment, Chinese Academy of Sciences, Chengdu, 610041, China
[b] School of Geography, Earth and Environmental Sciences, University of Plymouth, Plymouth, Devon, PL4 8AA, UK
[c] Department of Resources and Environmental Engineering, Sichuan Water Conservancy Vocational College, Chengdu, 611231, China

## ARTICLE INFO

*Keywords:*
Beryllium-7
Spatial variability
Reference site
Microscale
Fallout radionuclides
Sediment tracer

## ABSTRACT

Quantitative assessment of soil erosion and deposition rates using fallout radionuclides (FRNs), including Beryllium-7 ($^{7}$Be), requires establishment of a reliable reference inventory i.e. the inventory of a non-eroding point. Little information, however, is currently available on the microscale spatial variability of $^{7}$Be inventory within reference sites. This is important information to inform sample design and replication, and in addition, to evaluate the uncertainty of derived soil redistribution data. In this study, soil samples were taken systematically at grid points on a 5 m × 12 m experimental reference plot with a bare soil surface, at two sampling occasions (2019 and 2021) in southwest China. $^{7}$Be activities were measured to explore the potential variability of $^{7}$Be inventory at the microscale. To determine possible causes of $^{7}$Be inventory variation, physicochemical characteristics including organic matter content (OM), pH, cation exchange capacity (CEC) and grain size compositions were analyzed at each sample location. $^{7}$Be inventories for the two periods were estimated at 211.1 $\pm$ 20.0 and 456.1 $\pm$ 43.8 Bq m$^{-2}$ (mean $\pm$ 2 SEM, $n = 44$), with coefficients of variation of 31.4 and 31.9% for the 2019 and 2021 sampling cases, respectively. No significant correlations were observed between $^{7}$Be activity and the measured soil compositional properties, suggesting observed spatial variability is primarily a result of random variation due to rainsplash and other processes, although sampling and measuring processes may contribute some uncertainties. Using the traditional method, ca. 40 independent reference samples are required to estimate the mean $^{7}$Be inventory, i.e. to represent input across the site, with an allowable error of 10% at 95% confidence, while application of a bootstrap approach suggests that ca. 28 would be adequate under similar accuracy. Overall, results of this study emphasize that the simple assumption of uniform distribution of $^{7}$Be across the reference area needs detailed examination on a case-by-case basis, if this radionuclide is to be used effectively to assess patterns and rates of soil redistribution from field to hillslope scale.

## 1. Introduction

Quantifying the magnitude and spatial distribution of soil redistribution rates has long been recognized as essential requirement for improved understanding of catchment sediment budget and effective soil and sediment management plans. The past several decades have witnessed successful application of fallout radionuclides (FRNs) including $^{137}$Cs, $^{210}$Pb$_{ex}$ and $^{7}$Be, to trace soil redistribution caused by erosion in a wide range of environments (IAEA, 2014). Assessment of rates and patterns of soil erosion and deposition using FRNs as tracers is commonly based on a comparison of the inventory (areal activity, Bq m$^{-2}$) of FRNs within a specified point or area with that for a local, undisturbed site, where neither erosion nor deposition has occurred and the FRN inventory reflects the total cumulative fallout input (i.e. reference inventory). Depletion or accumulation of FRN inventory at that sampling point relative to the reference value will provide evidence of soil erosion or deposition. A precise and reliable reference value therefore plays a crucial role in converting FRN inventories to rates of soil redistribution, since an inaccurate reference value will result in biased and unreliable results of erosion estimation (Mabit et al., 2008) and/or a greater uncertainty in derived values.

$^{7}$Be is a natural fallout radionuclide produced in the stratosphere and troposphere by the cosmic ray spallation of nitrogen and oxygen. Unlike man-made $^{137}$Cs, $^{7}$Be is continuously produced in the atmosphere. Its

---

[*] Corresponding author.
*E-mail address:* shizl@imde.ac.cn (Z. Shi).

https://doi.org/10.1016/j.jenvrad.2022.106978
Received 6 May 2022; Received in revised form 26 July 2022; Accepted 27 July 2022

input to the earth surface is predominantly associated with wet deposition (Wallbrink and Murray, 1994; Dovlete et al., 2021). Numerous studies in a wide range of environments have evidenced significant seasonal variations in $^{7}$Be fallout input from the atmosphere and its content in soils (e.g. Juri Ayub et al., 2009; Lohaiza et al., 2014; Esquivel et al., 2017). Under common rainfall and field conditions, $^{7}$Be is rapidly and stably adsorbed to soil particles upon fallout (Ryken et al., 2018b; Taylor et al., 2012). With a short half-life of 53.3 d, $^{7}$Be is typically concentrated within the upper millimeters (ca. 20 mm) of the soil surface. The shallow depth distribution of $^{7}$Be in soil and its short half-life makes it a useful tool to document soil and sediment redistribution associated with individual events or short periods (e.g. several weeks) of heavy rainfall where processes of sheetwash and shallow rill/inter-rill erosion dominate. Given that a large amount of annual soil loss is often associated with a limited number of extreme events (González-Hidalgo et al., 2009), information on rates and patterns of soil redistribution over short-term timescales provided by $^{7}$Be is of great value in developing effective soil conservation strategies especially in the context of climate change.

One of the major assumptions related to the use of $^{7}$Be as a sediment tracer is that prior to the target erosional event(s), $^{7}$Be is uniformly distributed across the area under investigation (Taylor et al., 2013; Walling, 2013). Only when this premise is met, can the changes in inventory at a given sampling point be attributed to the result of soil movement. However, to date this assumption has rarely been tested. Most importantly, existing evidence from $^{137}$Cs studies indicate that the commonly accepted assumption of uniform distribution across the reference area is not always met (Parsons and Foster, 2011) and sufficient number of samples must be taken to address such variability (Sutherland, 1996) and/or sampling strategies that integrate across wider areas adopted (Blake et al., 2009; Wallbrink and Croke, 2002).

Despite increasing attempts to use $^{7}$Be for documenting soil redistribution rates (Blake et al., 1999; de Rosas et al., 2018; Deumlich et al., 2017; Esquivel et al., 2021; Jha et al., 2015; Khodadadi et al., 2020; Li et al., 2016; Navas et al., 2008; Porto et al., 2016; Porto and Walling, 2014; Ryken et al., 2018c; Schuller et al., 2006, 2010; Sepulveda et al., 2008; Shi et al., 2011, 2013; Walling et al., 1999, 2009; Wilson et al., 2003), the spatial variability of $^{7}$Be at reference sites are under-investigated. Generally, two approaches have been used to determine the $^{7}$Be reference inventory at a given study area. The first involves the collection of shallow soil cores from a stable flat site adjacent to the study area. Using this method, replicate bulk cores are obtained and measured individually. The mean value of $^{7}$Be content (Bq m$^{-2}$) in soil can then be calculated to represent the reference value (e.g. Walling et al., 1999; Blake et al., 1999). Appling this sampling scheme the spatial variability of $^{7}$Be at the reference site can be assessed. However, in locations where the spatial variability is significant, a sufficient number of samples must be taken and the variability between them quantified and accounted for in subsequent modelling (Blake et al., 2009; Mabit and Blake, 2019). The increased sample size to gain representative evaluation of the mean is a major challenge with regard to laboratory capacity, since $^{7}$Be should be measured soon after sample collection due to its short half-life. It is noted that where bulk-core sampling strategies are used, at least one additional sectioned core is required to provide $^{7}$Be depth distribution in soil profile. This is an essential step to determining the relaxation mass depth ($h_0$, kg m$^{-2}$), another key parameter in the conversion models and of course representation of the soil profile being studued is essential (Mabit and Blake, 2019).

Most other attempts to establish the $^{7}$Be reference inventory (e.g. Schuller et al., 2006; Sepulveda et al., 2008; Walling et al., 2009; Shi et al., 2011; Porto and Walling, 2014) have adopted an alternative sampling approach. In these studies, several soil cores were collected from the reference site and sectioned into 2 or 3 mm slices using a special coring device, for example the Fine Increment Soil Collector (Mabit et al., 2014). The slices representing specific depth increments were then bulked to provide a single composite sample for measurement. Thus, the total inventory at that reference site can be readily calculated from the direct measurements of $^{7}$Be activity concentration (Bq kg$^{-1}$) in each depth increment, combining with the information on bulk density and depth increment. Since multiple cores were collected from different points in the reference site, representative depth distribution and total inventory can be obtained. However, the use of spatially-averaged values means that spatial variabilities associated with depth distribution and inventory could not be quantified.

Owing to rapid radioactive decay of $^{7}$Be and generally limited analytical resources (e.g. gamma detectors), sample numbers are often constrained in most $^{7}$Be tracing studies. Given potential spatial variability of $^{7}$Be inventory in reference locations, an important question for $^{7}$Be soil erosion estimation is how many points must be sampled to establish a reliable reference level, i.e. a reliable estimate of the overall fallout input to the study area. A commonly used method to determine the necessary size of samples is based on a simple statistical principle that the minimum number of samples needed is proportional to the square of the coefficient of variation with a specified allowable error (see Section 2.4 for more details). Nevertheless, the usefulness of this method is sometimes limited because it requires an independent and normal distribution of sample values (Wang et al., 2008).

An alternative way to estimate the necessary size of samples is the bootstrap approach. Using this method, the sample collected is treated as if it is the population, and Monte Carlo sampling (with replacement) is applied to create an empirical estimate of the statistic's sampling distribution (Sutherland, 1998). The advantage of the bootstrap method over the traditional one is that it does not need to make any assumption about the population distribution (Wang et al., 2008), and therefore represents a useful tool to estimate the necessary sample size, particularly when limited samples were collected (Sutherland, 1998). To resolve some of these complexities, the objectives of this study were to (1) evaluate the spatial variability of $^{7}$Be inventory at a reference site in southwest China, (2) explore the possible causes of the observed variability of $^{7}$Be, and (3) determine the number of reference samples needed to provide a representative inventory value under certain accuracy.

## 2. Materials and methods

### 2.1. Site description

The study site was located at a field observation station in Zhongxian County, Chongqing Municipality, China (latitude 30°25′22″N, longitude 108°10′25″E) (Fig. 1a). The local area is characterized by a subtropical monsoonal climate with an average annual temperature of 19.2 °C. Mean annual precipitation is approximately 1110 mm during the past 20 years, with most of it falling from April to October. The soils are purple soils with a silt loam texture, developed on the products of rapid weathering of sandstones, siltstones and mudstones of the Jurassic Shaximiao Group (J$_2$s). These have been classified as Orthic Entisols in the Chinese Soil Taxonomic System, Regosols in the FAO Taxonomy and Entisols in the USDA Taxonomy. The "purple" color of the soils has been attributed to the presence of $Fe_2O_3$ and MnO as an adhesive film on the surface of the particles comprising the parent materials. Due to rapid physical weathering processes, the soils are lithologic soils without distinct pedogenic horizons (Shi et al., 2017).

### 2.2. Sample collection

An experimental plot 5 m wide and 12 m long, with a flat surface was established as the reference site for this investigation (Fig. 1b). The plot was originally installed in 2016 and was subsequently maintained in undisturbed and bare condition. A digital rain gauge located in close proximity to the plot provides a continuous record of rainfall with a resolution of 0.2 mm.

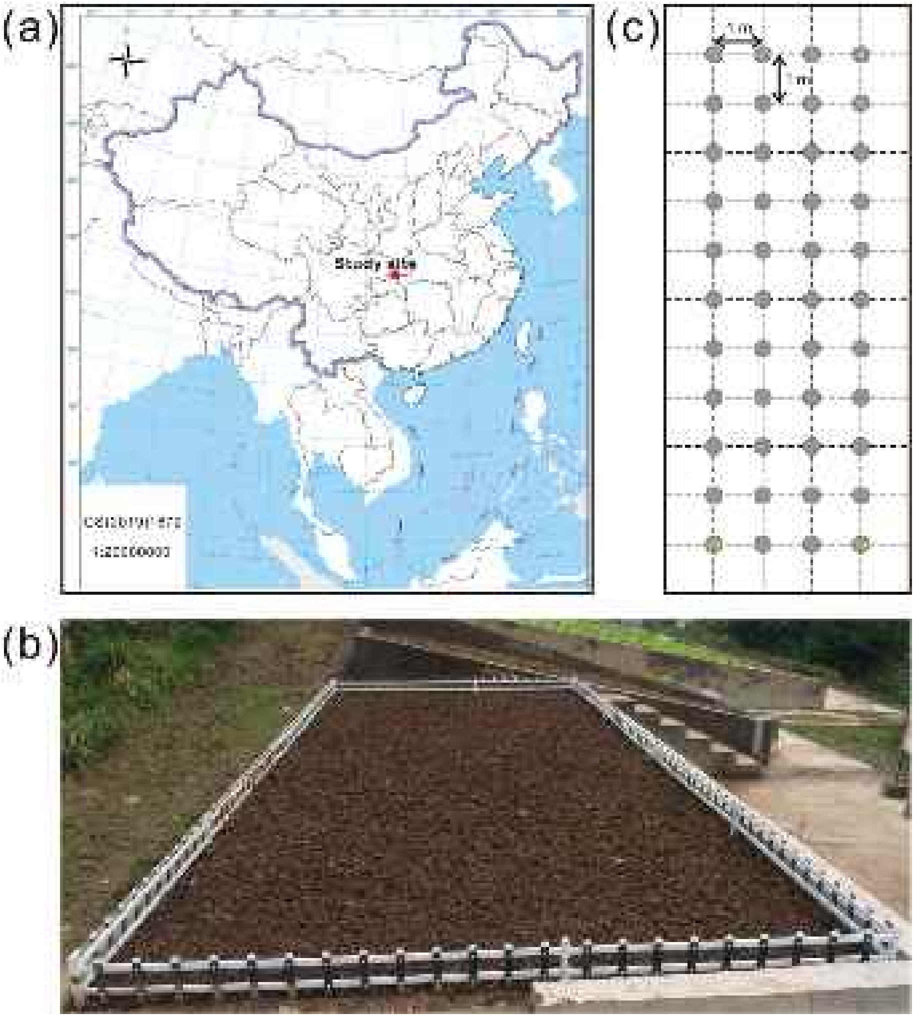

**Fig. 1.** Location of the study site (a), photograph of the experimental plot (b) and sampling design for the 4 × 11 rectangular grid with enumerated point numbers (c).

Soil sampling was carried out on May 15, 2019 and May 18, 2021, respectively, at the beginning of the rainy season of the study area (Fig. 2). A systematic grid sampling design was adopted to collect soil samples. The sampling points were located at the intersections of a 4 × 11 grid with a distance of 1 m between sampling points (Fig. 1c). At each point, one soil core was sampled using a stainless steel cylinder with an internal diameter of 10 cm (78.54 $cm^2$ cross-section area) and a depth of 3 cm. Previous investigations have shown that for the soil and rainfall environments at the study area, a sampling depth of 3 cm is sufficient to include the total $^7$Be inventory in soil profile and to avoid excessive dilution of $^7$Be by soils from below the depth containing $^7$Be (Shi et al., 2011, 2013). A total of 44 soil samples were obtained for each sampling occasion.

### 2.3. Laboratory procedures

After collection, soil samples were oven-dried at 60 °C for 24 h and subsequently disaggregated manually by use of a mortar and pestle. Samples were then dry sieved through a 2 mm mesh and homogenized for further analysis. $^7$Be activity concentrations in soil samples (<2 mm) were determined by measuring its gamma emission at 477.6 keV using a GMX40P4 coaxial high purity germanium (HPGe) detector coupled to a multi-channel analyzer. In order to minimize the uncertainties associated with the precision of $^7$Be measurement, all samples were measured on a single detector (Owens and Walling, 1996). The detector was calibrated using mixed sources with similar matrix and geometry and the relative efficiency was 40% at 1.33 MeV. Count times were typically >40,000 s, providing a measurement error of ca. 15% at the 95% level of confidence. All $^7$Be mass activities were decay-corrected to the date of sampling. For each sampling point, $^7$Be areal activity, i.e. inventory, (Bq $m^{-2}$) was calculated by multiplying the measured $^7$Be activity (Bq $kg^{-1}$) by the <2 mm dry mass (kg), divided by the core surface area ($m^2$).

Subsamples were taken to analyze the organic matter content, pH, cation exchange capacity (CEC) and grain size composition. Organic matter in soil was determined by loss-on-ignition at 850 °C for 2 h. Soil pH was measured in distilled water extracts (1:2.5 w/v) using a pH-meter (S210 SevenCompact, METTLER TOLEDO). The CEC was measured via the method of ammonium acetate centrifugal exchange. Grain size composition (clay <2 μm, silt 2–63 μm, sand >63 μm) was obtained using a Malvern Mastersizer 2000 laser diffraction device. Prior to particle size analysis, the samples were treated with 10% $H_2O_2$ to remove organic matter and 10% HCl to remove $CaCO_3$ before being dispersed by use of 0.5 mol $L^{-1}$ sodium hexametaphosphate solution and 2-min ultrasonic agitation.

### 2.4. Data analysis

Data sets were tested for normality using the Shapiro-Wilk test. To assess the difference of measured values between the two sampling cases, the Mann-Whitney *U* test was applied. The Spearman rank

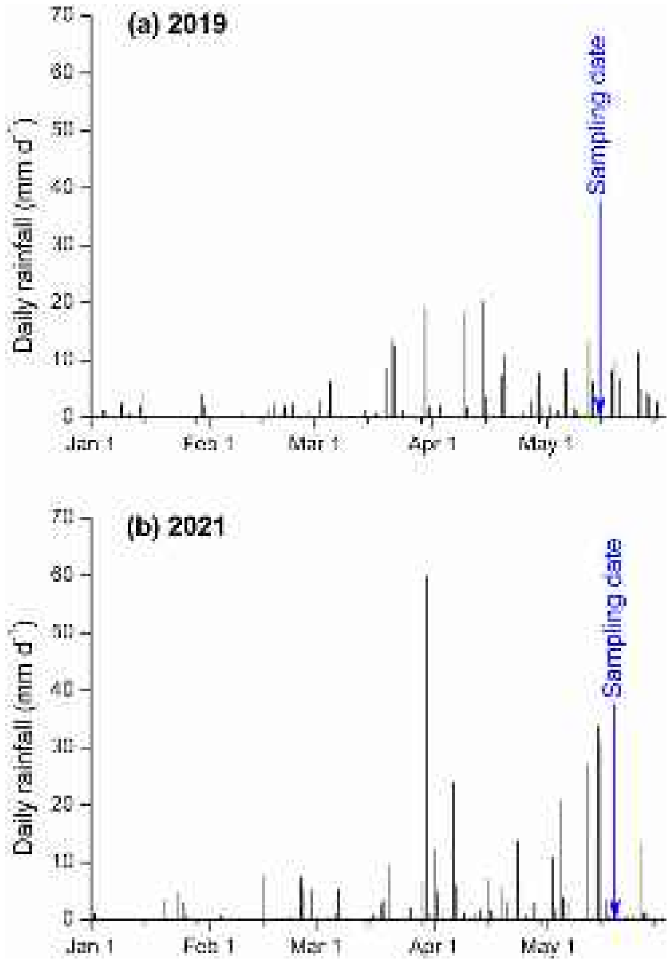

**Fig. 2.** Daily rainfall records for the study site with the blue arrows showing the dates of soil sampling.

correlation analysis (two-tailed test) was then used to determine possible relationships between $^7$Be activity concentrations and other measured soil properties.

The minimum number of samples needed ($N$) to estimate the population mean of the $^7$Be reference inventory within a specific level of confidence can be calculated using traditional criteria (Bazshoushtari et al., 2016; Mabit et al., 2012; Nolin et al., 1993; Sutherland, 1996; Zhang et al., 2019):

$$N = [\frac{t_{(\alpha,n-1)} \cdot CV}{AE}]^2 \tag{1}$$

where $t$ is the Student's $t$-value with $n$-1 degrees of freedom at the α confidence level, where $n$ is the number of samples used to calculate CV, $CV$ is the coefficient of variation (decimal fraction) and is defined as the standard deviation divided by arithmetic mean, and $AE$ is the allowable error (decimal fraction).

The application of Equation (1) assumes that observations are not only normally, as in our case, but also randomly distributed. The latter means that samples taken to provide an effective average should not be spatially auto-correlated (Sutherland, 1996). To verify the randomness of $^7$Be inventory at the reference area, the rank von Neumann's ratio test (Bartels, 1982) was used and the $^7$Be values in each row ($n = 4$) and each column ($n = 11$) were tested separately. This test was implemented by use of the '*randtests*' package in *R* (Mateus and Caeiro, 2014).

For the bootstrap resampling approach, the random samples were obtained using the tool of Resampling Stats Add-in for Excel (Statistics.com, LLC). In brief, a subsample of size $n$ ($n$ = 4, 8, 12, 16, 20, 24, 28, 32, 36, 40) was drawn randomly from the total 44 observations. Each subsample of size $n$ was resampled 1000 times, with replacement (i.e. observations are put back in the population after each draw for possible future reselection), and a mean value was calculated each time. The 1000 means were ranked and the 2.5th and 97.5th percentiles of the bootstrap mean distribution were used to determine the 95% confidence intervals around the mean for the reference location. Relative errors between the mean of 1000 means for each subsample and the mean of the total 44 observations were also calculated.

## 3. Results and discussion

### 3.1. Microscale variability of $^7$Be at the reference site

The summary statistics of the measured $^7$Be activities are presented in Table 1. The Shapiro-Wilk Normality test indicated that $^7$Be activities were normally distributed for both data sets (Supplemental Table S1). In the case of 2019, $^7$Be mass activities ranged from 2.5 to 10.9 Bq kg$^{-1}$ with an average of 6.4 ± 2.0 Bq kg$^{-1}$ (mean ± SD) and a CV of 31.3%. The areal activities ranged between 82.7 and 417.6 Bq m$^{-2}$ with an average of 211.1 ± 66.2 Bq m$^{-2}$ and CV of 31.4%. One of the sampling points (point 44 in Fig. 1c) produced an areal activity of 417.6 Bq m$^{-2}$, which was obviously higher (> mean + 3SD) than the others. A boxplot of $^7$Be areal activity for 2019 further identified this outlier (Supplemental Fig. S1). With this value removed from the data set, the recalculated mean areal activity in 2019 was 206.3 ± 58.7 Bq m$^{-2}$ with CV declining to 28.5%. However, discarding such an observation is somewhat arbitrary, especially when variabilities are being explored. Thus, this value was retained and used for subsequent data treatment and analysis.

A greater $^7$Be content was detected in the sampled soils in 2021, with mass activities ranged between 5.6 and 22.1 Bq kg$^{-1}$ and areal activities between 213.9 and 775.6 Bq m$^{-2}$. Mean areal activity was 456.1 ± 145.5 Bq m$^{-2}$ (CV = 31.9%) and no outliers were found. The Mann-Whitney $U$ test demonstrated significant differences in $^7$Be activity between the two sampling cases (Supplemental Table S2). The higher $^7$Be activity in soils in 2021 than 2019 can be explained by higher rainfall amounts of 384.0 mm from January 1 to May 18, 2021, compared with that of 225.4 mm from January 1 to May 15, 2019 (Fig. 2). Numerous studies have demonstrated that $^7$Be fallout input to the Earth's surface is dominated by wet deposition and $^7$Be deposition flux is commonly positively correlated with precipitation amount (e.g. Doering and Akber, 2008; Dovlete et al., 2021; Dueñas et al., 2017; Juri Ayub et al., 2009; Pham et al., 2013; Zhang et al., 2013). The impact of any pre-existing $^7$Be within the soil before January 1 on its content at the dates of sampling can assumed to be minimal, considering little rainfall and thus low fallout input in preceding dry months, as well as the rapid radioactive decay of $^7$Be.

While it is difficult to make direct comparison between $^7$Be reference values for different sites due to seasonal and regional variability, a comparison of variabilities within reference locations can be useful to understand the spatial patterns and dynamics of this radionuclide in different soils. Unfortunately, to date there is relatively limited information on the spatial variation of $^7$Be in reference areas. In the UK, Blake et al. (1999) reported a reference inventory of 512 ± 33 Bq m$^{-2}$ (CV = 6.4%), which reflects a generally uniform distribution of $^7$Be over grass covered soil. However, in a burnt forested soil in Australia, the mean reference inventory for $^7$Be was found to be 266 ± 33 Bq m$^{-2}$ based on 20 individual cores underneath a burnt forest cover (Blake et al., 2009). Given that the error of ±33 Bq m$^{-2}$ was the standard error of the mean rather than the standard deviation, a much higher degree of variation with CV of nearly 55% can be calculated in this heterogenous fallout environment. This high spatial variability, comparing with those in commonly used bare reference soils, may be attributed at least partially to the effects of canopy interception of initial fallout, the spatial variability of throughfall, and the localized redistribution of ash by wind and

**Table 1**

Summary statistics of $^{7}$Be mass activity, areal activity and some basic physicochemical properties of the soil samples.

| Parameter | $^{7}$Be mass activity (Bq kg$^{-1}$) | $^{7}$Be areal activity (Bq m$^{-2}$) | pH | OM (%) | CEC (cmoL kg$^{-1}$) | Clay (%) | Silt (%) | Sand (%) |
|---|---|---|---|---|---|---|---|---|
| **15 May 2019 (n = 44)** | | | | | | | | |
| Minimum | 2.5 | 82.7 | 7.9 | 0.8 | 18.7 | 1.4 | 59.0 | 10.4 |
| Maximum | 10.9 | 417.6 | 8.4 | 1.2 | 21.7 | 4.5 | 86.9 | 39.2 |
| Mean | 6.4 | 211.1 | 8.1 | 1.0 | 19.6 | 2.7 | 73.0 | 24.3 |
| Median | 6.6 | 211.7 | 8.1 | 1.0 | 19.5 | 2.7 | 72.9 | 24.4 |
| SD | 2.0 | 66.2 | 0.1 | 0.1 | 0.6 | 0.7 | 7.0 | 7.4 |
| SEM | 0.3 | 10.0 | 0.0 | 0.0 | 0.1 | 0.1 | 1.1 | 1.1 |
| CV | 31.3 | 31.4 | 1.2 | 10.0 | 3.1 | 25.9 | 9.6 | 30.5 |
| 95% CI | 5.8–7.0 | 190.9–231.2 | 8.1–8.2 | 1.0–1.0 | 19.4–19.8 | 2.5–2.9 | 70.8–75.1 | 22.1–26.6 |
| **18 May 2021 (n = 44)** | | | | | | | | |
| Minimum | 5.6 | 213.9 | 6.6 | 0.6 | 16.0 | 1.8 | 64.7 | 11.6 |
| Maximum | 22.1 | 775.6 | 8.2 | 1.5 | 19.2 | 4.0 | 84.4 | 33.5 |
| Mean | 12.9 | 456.1 | 7.1 | 0.9 | 17.3 | 2.6 | 73.4 | 24.0 |
| Median | 13.2 | 460.4 | 7.1 | 0.9 | 17.2 | 2.5 | 73.3 | 24.1 |
| SD | 4.4 | 145.5 | 0.4 | 0.2 | 0.7 | 0.4 | 4.1 | 4.4 |
| SEM | 0.7 | 21.9 | 0.1 | 0.0 | 0.1 | 0.1 | 0.6 | 0.7 |
| CV | 34.1 | 31.9 | 5.6 | 22.2 | 4.0 | 15.4 | 5.6 | 18.3 |
| 95% CI | 11.5–14.2 | 411.8–500.3 | 7.0–7.2 | 0.9–1.0 | 17.1–17.6 | 2.5–2.8 | 72.2–74.7 | 22.6–25.3 |

OM: organic matter content; CEC: cation exchange capacity; SD: standard deviation; SEM: standard error of the mean; CV: coefficient of variation; CI: confidence interval for the mean (%).

rainsplash. Some other studies provided CVs that fall within the range of the above values. For example, Iurian et al. (2013) documented a CV of 19% from 10 sampling points whereas Ryken et al. (2018a) reported a CV of 36% within their 400 m$^{2}$ reference site.

Table 1 lists summary statistics of the measured physicochemical properties of the soils. The CV values indicate that pH and CEC were the most consistent properties at the study site. The silt (2–63 μm) contents also exhibit low variability with CVs not exceeding 10%. This was expected because silt is the dominant particle size fraction of the study soil. Other soil properties (OM, clay and sand contents) fall generally within the moderate variability category (i.e., CV = 15–35%) of Wilding and Drees (1983). Significant differences were noted (Mann-Whitney *U* test) in soil pH, OM and CEC between the two data sets (Supplemental Table S2), with measured values lower in 2021 than those in 2019 (Supplemental Fig. S1). For particle size characteristics, however, no significant differences were found between the two study cases.

### 3.2. Possible causes of the observed variability of $^{7}$Be

Although factors affecting $^{7}$Be depositional fluxes at macro- and mesoscales have been well investigated in previous studies, little information is currently available at the microscale (Taylor et al., 2013). In Australia, Wallbrink and Murray (1996) documented a CV of 5–18% for $^{7}$Be inventory in undisturbed, near-level (slope $<5^{\circ}$) bare soils. With no observation of soil redistribution at the site, the authors attributed this variation to real differences in effective fallout and immediate relocation of $^{7}$Be prior to sorption. Further, they inferred that such relocation was probably a result of differences in soil properties such as texture, density, pH, and CEC over scales of 1–100 cm (Wallbrink and Murray, 1996).

The Spearman rank correlation analysis suggests that $^{7}$Be was not significantly correlated with any soil physiochemical characteristics (Supplemental Table S3), indicating that in this study the spatial pattern of $^{7}$Be at the reference site cannot be explained by differences in these soil properties. Similar findings were reported for fallout $^{137}$Cs by Sutherland (1991).

Since the samples in this study were taken from a bare, flat and very small area, the effects of meteorological conditions (e.g. variation of rainfall and wind flow) and vegetation interception and redistribution on $^{7}$Be input into soils should not be responsible for the occurrence of the spatial variability. In this context, the observed spatial variation of $^{7}$Be activity is more likely a result of random spatial variability that originated from differences in soil infiltration capacity between sampling points, micro-topography introduced by soil clods and small hollows, as well as local redistribution of soil particles by rain splash (Blake et al., 2019) where size selectivity of transport could potentially have a major influence on localized activity concentration (Taylor et al., 2014). Nevertheless, it is important to point out that the variability presented is a combination of random environmental variability and errors inherently included in sampling and measuring processes.

Owens and Walling (1996) indicated that during field sampling campaigns, the surface area is unlikely to be exactly the same for each of the samples collected, even if a narrow core tube (38 cm$^{2}$ surface area) was applied. Thus, they stated that the sampling variability is a function of the surface area over which the samples are collected. The authors also cited a work by Foster et al. (1994), in which a maximum error associated with core tube deformation as a result of sampling stony soils was calculated to be ±5.5%. In our study, such source of variability related to the deformation of sampler can assumed to be minimal, since a stainless steel cylinder was used and no hard stones were encountered during sample collection. However, the presence of small soil clods and hollows at some of the sampling points means that a precise coring of 3 cm depth is impossible. Unfortunately, the uncertainty associated with sample collection, and thus its importance to the total variability, is quite difficult to quantify in this study.

Possible errors arising from the process of gamma spectroscopy measurement depend on the sample activity, counting time and detector efficiency (Owens and Walling, 1996). Higher sample activity and longer count time will generate lower measurement errors. Following the methods of Sully et al. (1987), Sutherland (1991) and Owens and Walling (1996), and assuming a sampling error of 5% and measurement error 15%, the uncertainties related to the processes of sampling and measurement are presented in Table 2. It is clear that, for both study cases, the variances associated with errors in sampling and measuring of the samples are considerably lower than the lower boundary of the 95% confidence limit for the population variance ($\sigma^{2}$). Therefore, it can be concluded that the random spatial variation was the primary source of the observed total variability within the reference site. This result is consistent with the existing evidence for $^{137}$Cs (e.g. Lettner et al., 2000; Owens and Walling, 1996; Sutherland, 1991; Tsuiki and Maeda, 2012).

### 3.3. Determining the optimum sample size to establish a reliable $^{7}$Be reference level

Results of the rank von Neumann's ratio test confirmed that $^{7}$Be variations for both study cases were random ($p > 0.05$) and the use of Equation (1) is therefore appropriate. Fig. 3 plots the number of samples required to estimate the mean $^{7}$Be inventory against different allowable errors and confidence levels. Results indicate that at a confidence level

**Table 2**

A comparison of uncertainties related to soil sampling and $^{7}$Be measurements.

| Sampling date | 15 May 2019 | 18 May 2021 |
|---|---|---|
| $N$ | 44 | 44 |
| $m$ (Bq m$^{-2}$) | 211.1 | 456.1 |
| $s$ (Bq m$^{-2}$) | 66.2 | 145.5 |
| $s^2$ (Bq m$^{-2}$) | 4382.4 | 21170.3 |
| $S_e$ (%) | 5.0 | 5.0 |
| $S_e$ (Bq m$^{-2}$) | 10.6 | 22.8 |
| $S2\ s$(Bq m$^{-2}$) | 27.9 | 130.0 |
| $M_e$ (%) | 15 | 15 |
| $M_e$ (Bq m$^{-2}$) | 31.7 | 68.4 |
| $S2\ m$ (Bq m$^{-2}$) | 250.7 | 1170.2 |
| 95% CL of $\sigma^2$ (Bq m$^{-2}$) | 2992–7035 | 14452–33986 |

$n$: number of samples; $m$: mean areal activity; $s$: standard deviation; $s^2$: sample variance; $S_e$: sampling error; $S2\ s$: variance due to sampling error, $= (S_e/2)^2$; $M_e$: measurement error; $S2\ m$: variance due to measurement error, $= (M_e/2)^2$; 95% CL of $\sigma^2$: 95% confidence limit for the population variance ($\sigma^2$), $= (n\text{-}1)\ s^2/\chi 2\ \alpha$, where $\chi 2\ \alpha$ is the chi-squared value based on $n$-1 degree of freedom at the confidence limit α (α = 0.025 for the upper limit and 0.975 for the lower limit).

of 95% with an allowable error of ±10%, 40 and 41 samples are necessary to achieve a reliable mean inventory for 2019 and 2021, respectively. If the extreme value of 417.6 Bq m$^{-2}$ in 2019 is discarded and a corresponding CV of 28.5% is used, the required sample size drops to 33.

Taking account of the rapid decay of $^{7}$Be, such a large sample size (note that this is just for characterizing the reference site) challenges the detection capacity in most laboratories. From practical and cost-effective considerations, a lesser but statistically sound number of reference samples would be preferred in $^{7}$Be based soil erosion studies. Given that $^{7}$Be variations in the reference site were random and no autocorrelations were found, a nonparametric bootstrap resampling approach was tested to evaluate whether or not a reliable mean inventory could be achieved by use of a smaller sample size under a comparable accuracy.

The statistics of the 1000 means determined from the bootstrap resampling approach are summarized in Table 3. The variations in the mean $^{7}$Be areal activity and the associated 95% confidence intervals for each subsample size are depicted in Fig. 4. For each individual sampling case, the bootstrap method generated nearly identical means for subsamples of various sizes. Relative errors from the means of sample “population” ranged between −0.02 ($n = 12$) and −0.53% ($n = 20$) for 2019, and between +0.06 ($n = 16$) and +0.89% ($n = 8$) for 2021. The minimal variation in the means of the 1000 bootstrap means was expected, since the original samples (i.e. population) were normally distributed. Moreover, the 1000 bootstrap replications are found to be generally appropriate to produce a representative mean and variance (DI Stefano et al., 2000; Sutherland, 1998), although it might not cover all possible combinations of samples (Wang et al., 2008).

Despite minor differences in estimated means, the 95% confidence intervals exhibit obvious variation in both sampling cases (Fig. 4). The greater the number of subsamples, the narrower the width of confidence intervals for means. It is interesting that, for both cases, the 95% confidence lines nearly intersect the ±10% error line at the sampler size $n \approx 28$. After that, the confidence intervals vary slightly with increase of $n$. This result indicates that a random sample of ca. 28 would have been adequate to yield a reliable estimate of the mean $^{7}$Be areal activity in our study site under a similar accuracy to the traditional method. This considerable reduction (30%) in the required number of samples highlights the effectiveness of the bootstrapping approach in establishing $^{7}$Be reference levels in a location with notable spatial variability.

One of the potential constraints in $^{7}$Be tracing investigations is the short half-life of this radionuclide, which means that sufficient gamma detection facilities should be available if a large number of samples are collected. To reduce the sample size but capture the variability in reference locations, taking replicate cores at each sampling point and bulking cores to provide spatially-integrated samples might be practically feasible (Blake et al., 2019). Herein, combining of soil samples probably reduces the spatial variability of reference inventory and allows more precise estimates of site *averages* to be made with fewer analyses, however, information on real field *variability* will be obscured (Wallbrink et al., 1994). Users need to bear these tradeoffs in mind when designing sampling strategies. A combination of the above optimization process and strategic sample integration is proposed as a pragmatic way forward.

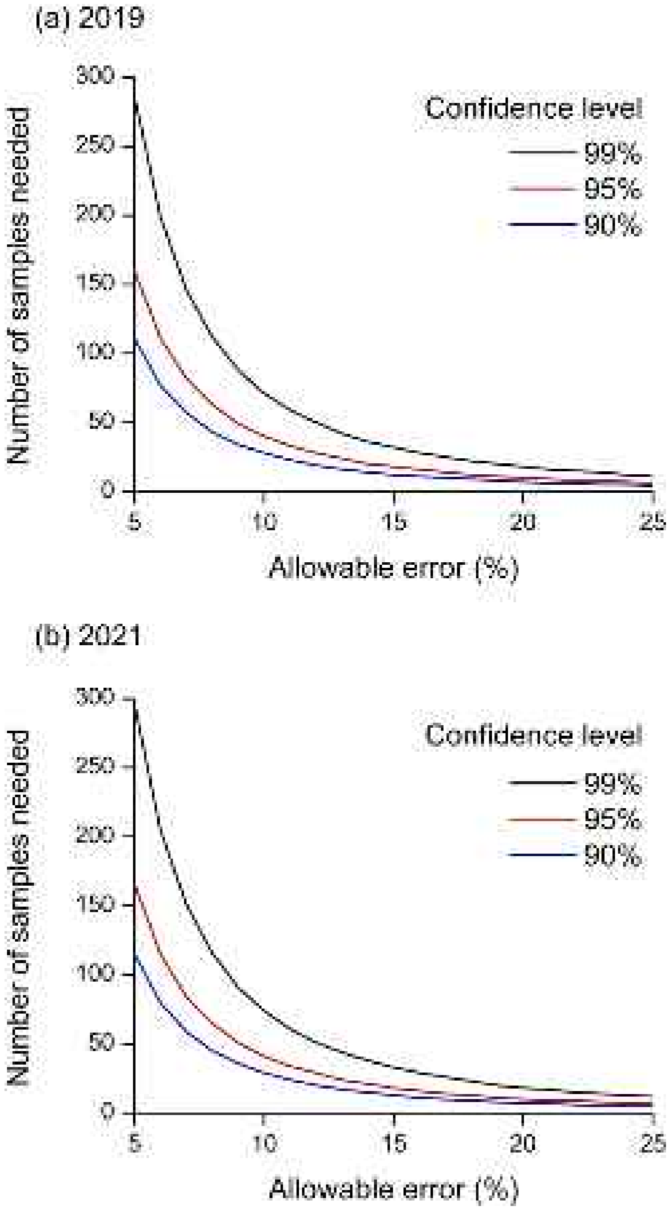

**Fig. 3.** Number of samples needed for a reliable estimation of mean $^{7}$Be inventory. The coefficients of variation (CV) used for calculation are 31.4% and 31.9% for 2019 (a) and 2021 (b), respectively.

## 4. Conclusions

The areal activity of $^{7}$Be was determined in a reference location with a silt loam soil texture. The $^{7}$Be areal activity was 211.1 ± 20.0 Bq m$^{-2}$ and 456.1 ± 43.8 Bq m$^{-2}$ (mean ± 2 SEM) for the 2019 and 2021 sampling cases, respectively. The spatial variability with a similar CV of ca. 31% for both cases suggests that the common assumption of uniform $^{7}$Be distribution at reference sites needs careful examination with

**Table 3**
Summary statistics of the 1000 means of $^7$Be areal activity determined from the bootstrap resampling approach (values in parentheses represent 2021 sampling occasion).

| Subsamples size (*n*) | Minimum | Maximum | Mean | Median | SD | SEM | CV |
|---|---|---|---|---|---|---|---|
| 4 | 114.1 (248.1) | 336.1 (683.8) | 211.2 (453.8) | 210.3 (453.6) | 33.0 (72.9) | 1.0 (2.3) | 15.6 (16.1) |
| 8 | 134.8 (299.7) | 297.9 (661.4) | 210.5 (460.2) | 209.3 (459.7) | 23.1 (51.5) | 0.7 (1.6) | 11.0 (11.2) |
| 12 | 151.3 (341.3) | 292.5 (604.9) | 211.1 (457.4) | 210.8 (457.6) | 19.1 (41.9) | 0.6 (1.3) | 9.1 (9.2) |
| 16 | 159.1 (338.8) | 267.7 (573.3) | 211.4 (456.4) | 210.9 (455.9) | 16.8 (37.0) | 0.5 (1.2) | 7.9 (8.1) |
| 20 | 161.4 (344.0) | 261.8 (557.3) | 210.0 (456.8) | 209.9 (457.7) | 14.3 (33.1) | 0.5 (1.0) | 6.8 (7.3) |
| 24 | 171.4 (354.6) | 254.4 (553.5) | 210.8 (454.7) | 211.0 (455.4) | 13.4 (30.3) | 0.4 (1.0) | 6.4 (6.7) |
| 28 | 173.9 (369.3) | 244.9 (549.9) | 211.4 (456.6) | 210.9 (456.6) | 12.0 (27.9) | 0.4 (0.9) | 5.7 (6.1) |
| 32 | 179.9 (379.5) | 246.1 (553.4) | 211.2 (455.5) | 211.0 (455.8) | 11.4 (25.1) | 0.4 (0.8) | 5.4 (5.5) |
| 36 | 178.1 (375.9) | 248.2 (524.9) | 210.6 (456.5) | 210.2 (455.8) | 10.6 (23.7) | 0.3 (0.7) | 5.0 (5.2) |
| 40 | 182.0 (384.6) | 239.6 (534.6) | 211.0 (456.6) | 210.9 (456.8) | 10.2 (22.9) | 0.3 (0.7) | 4.8 (5.0) |

SD: standard deviation; SEM: standard error of the mean; CV: coefficient of variation (%).

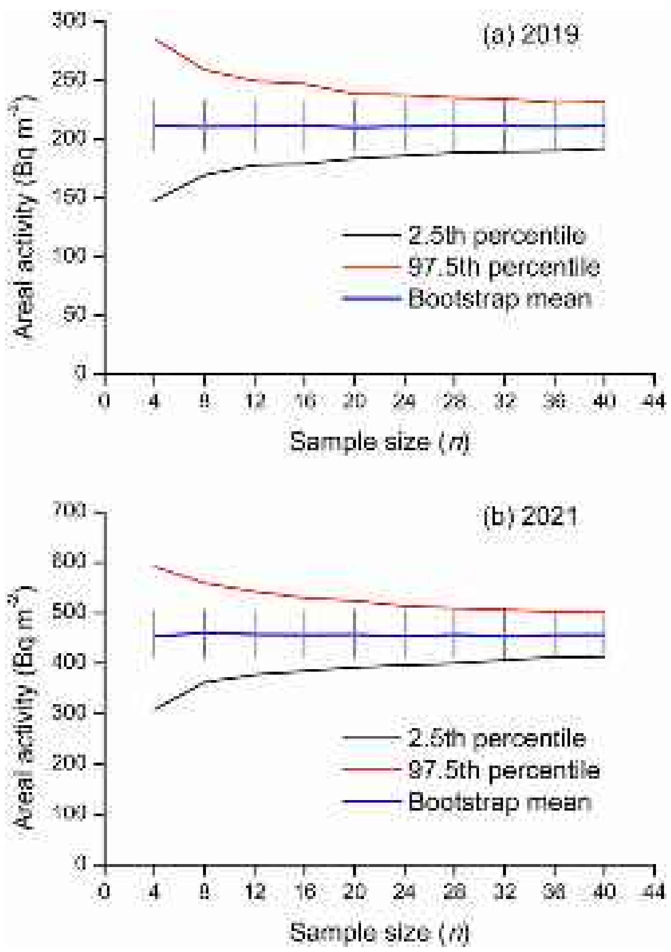

**Fig. 4.** Bootstrap mean and the 2.5th and 97.5th percentile values of the $^7$Be areal activity determined from the resampling method. The gray vertical lines show ±10% allowable error of the mean of the total 44 samples.

sampling regimes adapted accordingly to capture the true input to the site. There was no significant relationship between $^7$Be activity and the measured soil properties (i.e. OM, pH, CEC and grain size). The observed spatial variability is primarily a result of random variation due to rainfall-soil interactions although sampling and measuring processes may introduce some uncertainties. The required number of samples to establish a reliable reference level of $^7$Be at this site, at 95% confidence level with allowable error of ±10%, was estimated to be 40. The bootstrap resampling method, however, indicate that a sample size of ca. 28 would be adequate. In the cases where analytical resources are quite limited, taking spatially-integrated reference samples that formed by combining serval point samples may be more time- and cost-effective and practically feasible. But it should be recognized that using this method, the information on real field spatial variability will be masked and users need to pay due attention to limitations in this regard when propagating uncertainty.

## Declaration of competing interest

The authors declare that they have no known competing financial interests or personal relationships that could have appeared to influence the work reported in this paper.

## Data availability

Data will be made available on request.

## Acknowledgements

This work was supported by the "*Western Light*" program of Chinese Academy of Sciences (ZS) and the Joint UN FAO/IAEA Coordinated Research Project D1.50.18 "*Multiple Isotope Fingerprints to Identify Sources and Transport of Agro-Contaminants*" (WB).

## Appendix A. Supplementary data

Supplementary data to this article can be found online at https://doi.org/10.1016/j.jenvrad.2022.106978.

## References

Bartels, R., 1982. The rank version of von Neumann's ratio test for randomness. J. Am. Stat. Assoc. 77 https://doi.org/10.1080/01621459.1982.10477764.

Bazshoushtari, N., Ayoubi, S., Abdi, M.R., Mohammadi, M., 2016. Variability of $^{137}$Cs inventory at a reference site in west-central Iran. J. Environ. Radioact. 165 https://doi.org/10.1016/j.jenvrad.2016.09.010.

Blake, W.H., Taylor, A., Toloza, A., Mabit, L., 2019. How to design a be-7 based soil distribution study at the field scale: a step-by-step approach. In: Assessing Recent Soil Erosion Rates through the Use of Beryllium, vol. 7. https://doi.org/10.1007/978-3-030-10982-0_2. Be-7).

Blake, W.H., Wallbrink, P.J., Wilkinson, S.N., Humphreys, G.S., Doerr, S.H., Shakesby, R. A., Tomkins, K.M., 2009. Deriving hillslope sediment budgets in wildfire-affected forests using fallout radionuclide tracers. Geomorphology 104. https://doi.org/10.1016/j.geomorph.2008.08.004.

Blake, W.H., Walling, D.E., He, Q., 1999. Fallout beryllium-7 as a tracer in soil erosion investigations. Appl. Radiat. Isot. 51 https://doi.org/10.1016/S0969-8043(99)00086-X.

de Rosas, J.P., Esquivel, A.D., Martinez Heimann, D., Negri, A.E., Lohaiza, F., Valladares, D.L., Zavala, A.I., Huck, H., Juri Ayub, J., 2018. Using beryllium-7 to evaluate soil erosion processes in agricultural lands in semiarid regions of Central Argentina. Environ. Earth Sci. 77 https://doi.org/10.1007/s12665-018-7767-x.

Deumlich, D., Jha, A., Kirchner, G., 2017. Comparing measurements, $^7$Be radiotracer technique and process-based erosion model for estimating short-term soil loss from cultivated land in Northern Germany. Soil Water Res. 12 https://doi.org/10.17221/124/2016-SWR.

DI Stefano, C., Ferro, V., Porto, P., 2000. Applying the bootstrap technique for studying soil redistribution by caesium-137 measurements at basin scale. Hydrol. Sci. J. 45 https://doi.org/10.1080/02626660009492318.

Doering, C., Akber, R., 2008. Beryllium-7 in near-surface air and deposition at Brisbane, Australia. J. Environ. Radioact. 99 https://doi.org/10.1016/j.jenvrad.2007.08.017.

Dovlete, C., Sonoc, S., Osvath, I., Sima, O., 2021. Long term $^7$Be deposition in Romania. J. Environ. Radioact. 240 https://doi.org/10.1016/j.jenvrad.2021.106738.

Dueñas, C., Gordo, E., Liger, E., Cabello, M., Cañete, S., Pérez, M., Torre-Luque, P. de la, 2017. $^7$Be, $^{210}$Pb and $^{40}$K depositions over 11 years in Málaga. J. Environ. Radioact. 178–179. https://doi.org/10.1016/j.jenvrad.2017.09.010.

Esquivel, A.D., Moreira, R.M., Monteiro, R.P.G., Rochido Dos Santos, A.A., Valladares, D. L., Juri Ayub, J., 2021. Quantification of soil erosion using $^7$Be in a steep watershed used for natural grazing in Brazil. Isot. Environ. Health Stud. 57 (3), 316–331. https://doi.org/10.1080/10256016.2021.1918687.

Esquivel, A.D., Moreira, R.M., Monteiro, R.P.G., Dos Santos, A.A.R., Juri Ayub, J., Valladares, D.L., 2017. Wet deposition and soil content of Beryllium–7 in a micro-watershed of Minas Gerais (Brazil). J. Environ. Radioact. 169–170. https://doi.org/10.1016/j.jenvrad.2016.12.014.

Foster, I.D.L., Dalgleish, H., Dearing, J.A., Jones, E.D., 1994. Quantifying Soil Erosion and Sediment Transport in Drainage Basins; Some Observations on the Use of $^{137}$Cs. Var. Stream Eros. sediment Transp. Proc. Symp. Canberra, 1994.

González-Hidalgo, J.C., de Luis, M., Batalla, R.J., 2009. Effects of the largest daily events on total soil erosion by rainwater. An analysis of the usle database. Earth Surf. Process. Landforms 34. https://doi.org/10.1002/esp.1892.

IAEA, 2014. Guidelines for Using Fallout Radionuclides to Assess Erosion and Effectiveness of Soil Conservation Strategies. IAEA-TECDOC-1741.

Iurian, A.R., Toloza, A., Adu-Gyamfi, J., Cosma, C., 2013. Spatial distribution of $^7$Be in soils of Lower Austria after heavy rains. J. Radioanal. Nucl. Chem. 298 https://doi.org/10.1007/s10967-013-2683-8.

Jha, A., Schkade, U., Kirchner, G., 2015. Estimating short-term soil erosion rates after single and multiple rainfall events by modelling the vertical distribution of cosmogenic $^7$Be in soils. Geoderma 243–244. https://doi.org/10.1016/j.geoderma.2014.12.020.

Juri Ayub, J., Di Gregorio, D.E., Velasco, H., Huck, H., Rizzotto, M., Lohaiza, F., 2009. Short-term seasonal variability in $^7$Be wet deposition in a semiarid ecosystem of central Argentina. J. Environ. Radioact. 100 https://doi.org/10.1016/j.jenvrad.2009.08.001.

Khodadadi, M., Zaman, M., Mabit, L., Blake, W.H., Gorji, M., Bahrami, A.S., Meftahi, M., Porto, P., 2020. Exploring the potential of using $^7$Be measurements to estimate soil redistribution rates in semi-arid areas: results from Western Iran and Southern Italy. J. Soils Sediments 20. https://doi.org/10.1007/s11368-020-02701-4.

Lettner, H., Bossew, P., Hubmer, A.K., 2000. Spatial variability of fallout Caesium-137 in Austrian alpine regions. J. Environ. Radioact. 47 (1), 71–82. https://doi.org/10.1016/S0265-931X(99)00023-5.

Li, Z., Lu, Y., Nie, X., Huang, B., Ma, W., Liu, C., Xiao, H., 2016. Variability of beryllium-7 and its potential for documenting soil and soil organic carbon redistribution by erosion. Soil Sci. Soc. Am. J. 80 https://doi.org/10.2136/sssaj2015.11.0392.

Lohaiza, F., Velasco, H., Juri Ayub, J., Rizzotto, M., Di Gregorio, D.E., Huck, H., Valladares, D.L., 2014. Annual variation of $^7$Be soil inventory in a semiarid region of central Argentina. J. Environ. Radioact. 130 https://doi.org/10.1016/j.jenvrad.2014.01.006.

Mabit, L., Benmansour, M., Walling, D.E., 2008. Comparative advantages and limitations of the fallout radionuclides $^{137}$Cs, $^{210}$Pb$_{ex}$ and $^7$Be for assessing soil erosion and sedimentation. J. Environ. Radioact. https://doi.org/10.1016/j.jenvrad.2008.08.009.

Mabit, L., Blake, W., 2019. Assessing Recent Soil Erosion Rates through the Use of Beryllium-7. https://doi.org/10.1007/978-3-030-10982-0. Be-7).

Mabit, L., Chhem-Kieth, S., Toloza, A., Vanwalleghem, T., Bernard, C., Amate, J.I., González de Molina, M., Gómez, J.A., 2012. Radioisotopic and physicochemical background indicators to assess soil degradation affecting olive orchards in southern Spain. Agric. Ecosyst. Environ. 159 https://doi.org/10.1016/j.agee.2012.06.014.

Mabit, L., Meusburger, K., Iurian, A.R., Owens, P.N., Toloza, A., Alewell, C., 2014. Sampling soil and sediment depth profiles at a fine resolution with a new device for determining physical, chemical and biological properties: the Fine Increment Soil Collector (FISC). J. Soils Sediments 14. https://doi.org/10.1007/s11368-013-0834-8.

Mateus, A., Caeiro, F., 2014. An R implementation of several randomness tests. In: AIP Conference Proceedings. https://doi.org/10.1063/1.4897792.

Navas, A., Walling, D.E., Gaspar, L., Machin, J., 2008. Use of Beryllium-7 to Assess Soil Redistribution by Erosion in Two Contrasting Mediterranean Environments. IAHS-AISH Publication.

Nolin, M.C., Cao, Y.Z., Coote, D.R., Wang, C., 1993. Short-range variability of fallout $^{137}$Cs in an uneroded forest soil. Can. J. Soil Sci. 73 https://doi.org/10.4141/cjss93-040.

Owens, P.N., Walling, D.E., 1996. Spatial variability of caesium-137 inventories at reference sites: an example from two contrasting sites in England and Zimbabwe. Appl. Radiat. Isot. 47 https://doi.org/10.1016/0969-8043(96)00015-2.

Parsons, A.J., Foster, I.D.L., 2011. What can we learn about soil erosion from the use of $^{137}$Cs? Earth Sci. Rev. https://doi.org/10.1016/j.earscirev.2011.06.004.

Pham, M.K., Povinec, P.P., Nies, H., Betti, M., 2013. Dry and wet deposition of $^7$Be, $^{210}$Pb and $^{137}$Cs in Monaco air during 1998-2010: seasonal variations of deposition fluxes. J. Environ. Radioact. 120 https://doi.org/10.1016/j.jenvrad.2012.12.007.

Porto, P., Walling, D.E., 2014. Use of $^7$Be measurements to estimate rates of soil loss from cultivated land: testing a new approach applicable to individual storm events occurring during an extended period. Water Resour. Res. 50 https://doi.org/10.1002/2014WR015867.

Porto, P., Walling, D.E., Cogliandro, V., Callegari, G., 2016. Validating a mass balance accounting approach to using $^7$Be measurements to estimate event-based erosion rates over an extended period at the catchment scale. Water Resour. Res. 52 https://doi.org/10.1002/2015WR018136.

Ryken, N., Al-Barri, B., Blake, W., Taylor, A., Tack, F., Bodé, S., Boeckx, P., Verdoodt, A., 2018a. Impact of soil hydrological properties on the $^7$Be depth distribution and the spatial variation of $^7$Be inventories across a small catchment. Geoderma 318. https://doi.org/10.1016/j.geoderma.2017.12.036.

Ryken, N., Al-Barri, B., Blake, W., Taylor, A., Tack, F.M.G., Van Ranst, E., Bodé, S., Boeckx, P., Verdoodt, A., 2018b. Rapid and irreversible sorption behavior of $^7$Be assessed to evaluate its use as a catchment sediment tracer. J. Environ. Radioact. 182 https://doi.org/10.1016/j.jenvrad.2017.11.018.

Ryken, N., Vanden Nest, T., Al-Barri, B., Blake, W., Taylor, A., Bodé, S., Ruysschaert, G., Boeckx, P., Verdoodt, A., 2018c. Soil erosion rates under different tillage practices in central Belgium: new perspectives from a combined approach of rainfall simulations and $^7$Be measurements. Soil Tillage Res. 179 https://doi.org/10.1016/j.still.2018.01.010.

Schuller, P., Iroumé, A., Walling, D.E., Mancilla, H.B., Castillo, A., Trumper, R.E., 2006. Use of beryllium-7 to document soil redistribution following forest harvest operations. J. Environ. Qual. 35 https://doi.org/10.2134/jeq2005.0410.

Schuller, P., Walling, D.E., Iroumé, A., Castillo, A., 2010. Use of beryllium-7 to study the effectiveness of woody trash barriers in reducing sediment delivery to streams after forest clearcutting. Soil Tillage Res. 110 https://doi.org/10.1016/j.still.2010.07.004.

Sepulveda, A., Schuller, P., Walling, D.E., Castillo, A., 2008. Use of $^7$Be to document soil erosion associated with a short period of extreme rainfall. J. Environ. Radioact. 99 https://doi.org/10.1016/j.jenvrad.2007.06.010.

Shi, Z., Wen, A., Ju, L., Yan, D., 2013. A modified model for estimating soil redistribution on grassland by using $^7$Be measurements. Plant Soil 362. https://doi.org/10.1007/s11104-012-1280-x.

Shi, Z., Wen, A., Walling, D.E., Wang, Y., Chen, J., 2017. Exploring particle size selectivity effects during erosion of purple soils in Chongqing municipality, China. J. Soils Sediments 17. https://doi.org/10.1007/s11368-016-1619-7.

Shi, Z., Wen, A., Zhang, X., Yan, D., 2011. Comparison of the soil losses from $^7$Be measurements and the monitoring data by erosion pins and runoff plots in the Three Gorges Reservoir region, China. Appl. Radiat. Isot. 69 https://doi.org/10.1016/j.apradiso.2011.05.031.

Sully, M.J., Flocchini, R.G., Nielsen, D.R., 1987. Linear distribution of naturally occurring radionuclides in a mollic Xerofluvent1. Soil Sci. Soc. Am. J. 51 https://doi.org/10.2136/sssaj1987.03615995005100020002x.

Sutherland, R.A., 1998. The potential for reference site resampling in estimating sediment redistribution and assessing landscape stability by the caesium-137 method. Hydrol. Process. 12 https://doi.org/10.1002/(SICI)1099-1085(19980615)12:7<995::AID-HYP634>3.0.CO;2-F.

Sutherland, R.A., 1996. Caesium-137 soil sampling and inventory variability in reference locations: a literature survey. Hydrol. Process. 10 https://doi.org/10.1002/(SICI)1099-1085(199601)10:1<43::AID-HYP298>3.0.CO;2-X.

Sutherland, R.A., 1991. Examination of caesium-137 areal activities in control (uneroded) locations. Soil Technol. 4 https://doi.org/10.1016/0933-3630(91)90038-O.

Taylor, A., Blake, W.H., Couldrick, L., Keith-Roach, M.J., 2012. Sorption behaviour of beryllium-7 and implications for its use as a sediment tracer. Geoderma 187–188. https://doi.org/10.1016/j.geoderma.2012.04.013.

Taylor, A., Blake, W.H., Keith-Roach, M.J., 2014. Estimating Be-7 association with soil particle size fractions for erosion and deposition modelling. J. Soils Sediments 14. https://doi.org/10.1007/s11368-014-0955-8.

Taylor, A., Blake, W.H., Smith, H.G., Mabit, L., Keith-Roach, M.J., 2013. Assumptions and challenges in the use of fallout beryllium-7 as a soil and sediment tracer in river basins. Earth Sci. Rev. https://doi.org/10.1016/j.earscirev.2013.08.002.

Tsuiki, M., Maeda, T., 2012. Spatial variability of radioactive cesium fallout on grasslands estimated in various scales. Grassl. Sci. 58 https://doi.org/10.1111/grs.12005.

Wallbrink, P.J., Croke, J., 2002. A combined rainfall simulator and tracer approach to assess the role of Best Management Practices in minimising sediment redistribution and loss in forests after harvesting. For. Ecol. Manage. 170 https://doi.org/10.1016/S0378-1127(01)00765-4.

Wallbrink, P.J., Murray, A.S., 1996. Distribution and variability of $^7$Be in soils under different surface cover conditions and its potential for describing soil redistribution processes. Water Resour. Res. 32 https://doi.org/10.1029/95WR02973.

Wallbrink, P.J., Murray, A.S., 1994. Fallout of $^7$Be in south Eastern Australia. J. Environ. Radioact. 25 https://doi.org/10.1016/0265-931X(94)90074-4.

Wallbrink, P.J., Olley, J.M., Murray, A.S., 1994. Measuring Soil Movement Using $^{137}$Cs: Implications of Reference Site Variability. Var. Stream Eros. sediment Transp. Proc. Symp. Canberra, 1994.

Walling, D.E., 2013. Beryllium-7: the Cinderella of fallout radionuclide sediment tracers? Hydrol. Process. 27 https://doi.org/10.1002/hyp.9546.

Walling, D.E., He, Q., Blake, W., 1999. Use of $^7$Be and $^{137}$Cs measurements to document short- and medium-term rates of water-induced soil erosion on agricultural land. Water Resour. Res. 35 https://doi.org/10.1029/1999WR900242.

Walling, D.E., Schuller, P., Zhang, Y., Iroumé, A., 2009. Extending the timescale for using beryllium 7 measurements to document soil redistribution by erosion. Water Resour. Res. 45 https://doi.org/10.1029/2008WR007143.

Wang, C., Zuo, Q., Zhang, R., 2008. Estimating the necessary sampling size of surface soil moisture at different scales using a random combination method. J. Hydrol. 352 https://doi.org/10.1016/j.jhydrol.2008.01.011.

Wilding, L.P., Drees, L.R., 1983. Spatial variability and pedology. Pedogenes. soil Taxon. I 83–116.

Wilson, C.G., Matisoff, G., Whiting, P.J., 2003. Short-term erosion rates from a $^{7}$Be inventory balance. Earth Surf. Process. Landforms 28. https://doi.org/10.1002/esp.509.

Zhang, F., Zhang, B., Yang, M., 2013. Beryllium-7 atmospheric deposition and soil inventory on the northern Loess Plateau of China. Atmos. Environ. 77 https://doi.org/10.1016/j.atmosenv.2013.05.002.

Zhang, X.C., Polyakov, V.O., Liu, B.Y., Nearing, M.A., 2019. Quantifying geostatistical properties of $^{137}$Cs and $^{210}$Pb$_{ex}$ at small scales for improving sampling design and soil erosion estimation. Geoderma 334. https://doi.org/10.1016/j.geoderma.2018.08.002.